

# Ballasting plan optimization for Accuracy control on Offshore Floating Dock

Seungkyun Yeo<sup>1)</sup>, Kyungho Yoon<sup>1)</sup>, Phill-Seung Lee<sup>1)</sup>, Younghwa Hong<sup>2)</sup>, JiHye Cha<sup>2)</sup> and Hyun Chung<sup>1)</sup>

<sup>1)</sup> Division of Ocean Systems Engineering, Korea Advanced Institute of Science and Technology, Republic of Korea  
<sup>2)</sup> Institute of Industrial Technology, Samsung Heavy Industries, Republic of Korea

## Abstract

In this paper, we propose and validate an accuracy control system for an Offshore Floating Dock (OFD) developed by Samsung Heavy Industries (SHI). The OFD was developed for constructing offshore structures on floating docks, and has a rectangular shape. Since the offshore structures are very heavy, the erection of offshore blocks causes global and local deformations of the OFD, which in turn adversely affects the alignment of the erection blocks. We propose a ballast plan optimization system for accuracy control. The proposed system was used and validated with data from the Jack & Saint Malo (JSM) offshore plant project that was being constructed on the OFD.

## Keywords

accuracy control; optimization; metamodeling; offshore plants; building docks; ballasting plan;

## Introduction

In the shipbuilding industry, the capacity of the building docks is the most important element among those that determine the productivity of the shipyard. These days, Korean shipyards are in a strategic move to construct more offshore plants instead of ships. This requires new kinds of building docks specialized for construction of offshore plants and installations. However, it is a major and complicated investment decision for a shipyard to construct a new building dock onshore, an option prohibited by the limited land area in most shipyards.

The alternative solution that SHI chose was to develop and construct an OFD, which would be moored adjacent to the block erection platen in SHI Geje Shipyard. Unlike the conventional floating dock for ships, this OFD has a rectangular deck area suited for onboard construction of offshore plants and has matrix arrangement, as shown as Fig.1, of ballast tanks.

During the block erection process on a conventional floating dock (Kurniawan and Ma, 2009), the ballasting

operation is carefully controlled in order to compensate for deflection due to the weight of the blocks and to maintain the flatness of the floating dock. Since the floating dock bends most in the longitudinal direction, typical ship blocks are symmetric along the longitudinal axis, and the ballast tanks are arranged longitudinally. Under these conditions, experienced operators can perform the ballasting operation easily and intuitively.

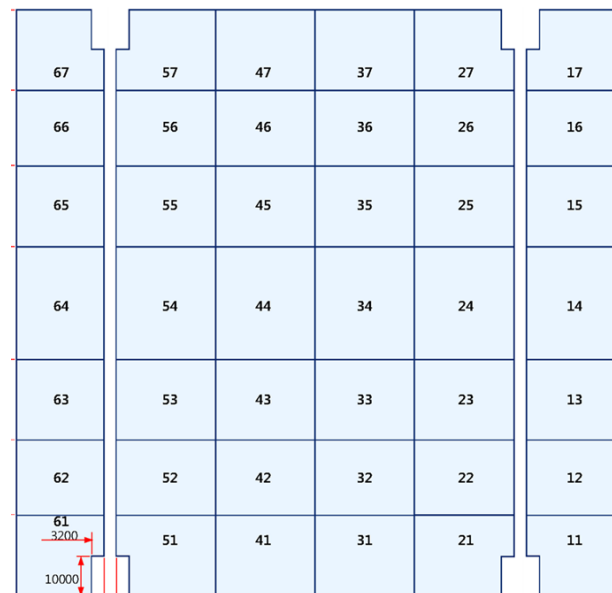


Fig. 1: Ballast tank arrangement

However, the OFD flexes longitudinally, and at the same time transversely, due to the non-uniform distribution of plant blocks. This requires more complicated calculations for ballasting plans to compensate for the deflections and to maintain the flatness of the deck.

The other issue in offshore block erection on an OFD is accuracy control. As the height of the column is 60-80 meters, even a minor deflection of the OFD deck can be magnified at the top of the columns. Because the 'mating' operation (raising the topside deck blocks to the top of the columns of the offshore installation hull) requires extreme accuracy, the ballasting plan must also control the OFD deck surface to assist accuracy during the mating operation.

In this work, we discuss the development of the OFD

ballasting-plan optimization-system for accuracy control of offshore block erection. In order to simulate the hydrostatic behavior of the OFD, an efficient and simplified numerical model was employed using plate and beam finite elements. The stiffness of the OFD has been determined using experimental tests designed to activate major strain energy modes and this stiffness was used in the numerical model. A gradient-based search method was applied for the search for an optimal solution, and then a meta-modeling technique was used to speed up the optimization time and compensate difference between simulation model and actual model.

The proposed system was applied to actual erection operations on the OFD at SHI Geoje Shipyard. The robotics research group at SHI measured deflections of the OFD and the measurement system was integrated with the proposed system. The real case experiment demonstrated that the proposed system successfully calculated and controlled the ballasting plan for accuracy control during offshore block erection on the OFD.

### Ballast plan optimization System

The optimization procedure for estimating the optimal ballast water plan (BWP) was divided into three parts (Fig. 2). In the first part, using an estimating optimal ballast water plan with FEM model, every erection step was subject to an initial BWP provided by SHI. The proposed system applied this BWP, which is provided by SHI, into the FEM model and allowed the FEM model figured out the deformation of the OFD deck. Then module of constraints estimate Trim, Heel, Draft by linear regression method as expressed in constraint section. Next was estimating the object function with the deformation data from the FEM model and constraints. If the object value was acceptable the proposed system advances to Part 2, otherwise, the BWP will be changed according to the steepest decent method. By iterative calculation, the proposed system finds the optimal ballast water plan.

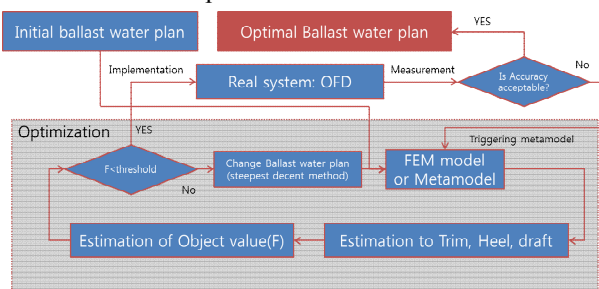


Fig. 2: Block diagram for optimization procedure

Part 2 involved implementation and measurement. SHI applied our optimal BWP estimated in Part 1. An automatic measurement system measured the accuracy of the offshore blocks and deformation of the OFD during ballasting. If the accuracy is acceptable, that BWP was the final optimal ballast water plan, if not, the proposed system starts Part 3.

The third part is metamodeling. If the accuracy of the operation on the real OFD is not acceptable, the proposed system makes a metamodel with data from the measurement systems. After making the metamodel, the

proposed system replaces the FEM model with the new metamodel, and then starts again with Part 1.

During actual erection of JSM, Part 3 could not be installed in the SHI system, so only Parts 1 and 2 were implemented. After the erection was done, we got measurement data from SHI and made a metamodel with the data. This allowed us to compare results from the metamodel with that from actual measurement data.

### Structural model

In this section, we introduce a highly efficient and simplified finite element model of the OFD, focused on the eighth step in construction of JSM offshore plant. As shown in Fig. 3, the physical OFD and erection blocks are modeled by plate and beam finite elements. The novel features of the present model are as follows:

- Only 468 DOFs are used for the whole OFD model.
- The erection model can be applied at arbitrary position of the OFD using localized a Lagrangian multiplier.
- An accurate global behavior can be calculated using an identified stiffness matrix.
- A simple anisotropic material model represents the number of stiffeners in the OFD.

In the following sections, we first present finite element model of the OFD with erection blocks Step 8, allowing for hydrostatic behavior. We then introduce an identification of the stiffness of the OFD through the major Eigen modes experimental tests.

### OFD model

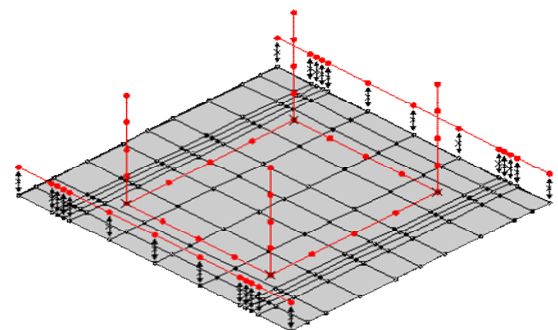
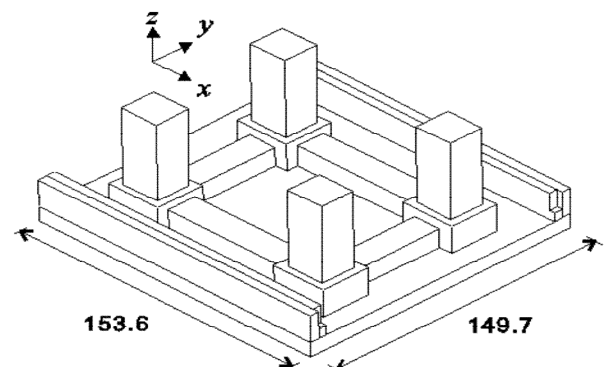
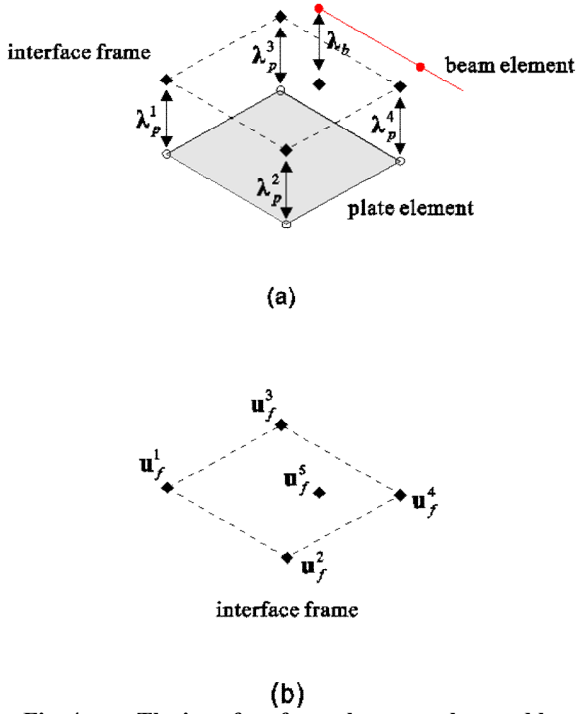


Fig. 3: Geometry of the physical OFD and its simplified finite element model with plate (gray) and beam (red) elements.

The OFD in step 8 is discretized by 120 plate and 56 beam finite elements as shown in Fig. 3. MITC4 plate elements with anisotropic constitutive relation are used



**Fig. 4:** The interface frame between plate and beam element. (a) The corresponding Lagrange multipliers applied at interface frame, (b) the corresponding displacements of interface frame.

For modeling the deck of the OFD (Bathe, 1996) (Lee PS and Bathe, 2005), Beam elements with eccentricity were used for modeling the sidewall of the OFD and the erection blocks (Yoon, 2005). In order to consider hydrostatic force, the following formulation, derived from a local equilibrium equation with a hydrostatic force term, are used for governing Eq. 1,

$$\int_V \tau_{ij} \delta \varepsilon_{ij} dV - \int_V p_i \delta u_i dV = \int_V f_i^b \delta u_i dV \quad (1)$$

To interconnect arbitrarily between the OFD and erection blocks, an interface frame was employed with interface frame displacements and localized Lagrange multipliers, as shown in Fig. 4 (Park, 2002). Then, five linear coupled equations could be derived, one plate equilibrium, one beam equilibrium, one interface frame equilibrium and two constraint equations among interface frame, plate and beam nodal displacements

$$\begin{bmatrix} K_p & 0 & C_p & 0 & 0 \\ 0 & K_b & 0 & C_b & 0 \\ C_p^T & 0 & 0 & 0 & -L_p \\ 0 & C_b^T & 0 & 0 & -L_b \\ 0 & 0 & -L_p^T & -L_b^T & 0 \end{bmatrix} \begin{bmatrix} u_p \\ u_b \\ \lambda_p \\ \lambda_b \\ u_f \end{bmatrix} = \begin{bmatrix} f_p \\ f_b \\ 0 \\ 0 \\ 0 \end{bmatrix} \quad (2)$$

where  $K_p$  is a stiffness matrix of plate elements,  $K_b$  is a stiffness matrix of beam elements,  $C_p$ ,  $C_b$ ,  $L_p$  and  $L_b$  are a Boolean matrix with shape functions. Eq. 2

allows interconnection for non-matching nodes.

### Identification of structural stiffness

In order to increase the accuracy of the proposed finite elements model, we performed experimental tests, and modified the x-directional and y-directional elastic moduli. The tests were designed to activate major strain energy modes, bending and twisting dominant test. Fig. 6a shows the bending dominated results, and that the X-directional elastic modulus has been determined. Fig. 6b shows the twisting dominated results, and that the y-directional elastic modulus has been determined. Fig. 6c and d show the results of the proposed model with the modified stiffness matrix.

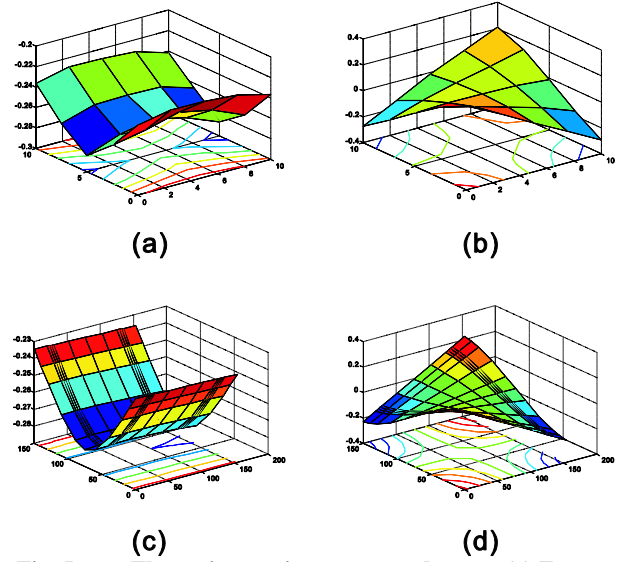


**Fig. 5:** The major strain energy mode tests. (a) Experimental results for bending dominant test, (b) experimental results for twisting dominant test, (c) modified numerical results for bending dominant test, (d) modified numerical results for twisting dominant test.

### Simulation and Optimization

OFD has an arrangement of 42 ballast tanks of various capacities as shown as Fig.1. During erection of offshore blocks on the deck of the OFD, the load of offshore blocks causes deformation of the OFD. If the ballast water in the tanks is managed so that deformation is properly controlled during erection of the blocks, we should easily be able to control the accuracy of the erection process to within acceptable tolerances.

The objective of this research was control of the accuracy in the matching of construction blocks of offshore plants, on an OFD developed by SHI. The source of this control was careful planning and distribution of ballast water into tanks on the OFD. Finding a BWP to satisfy the tolerances for matching the offshore blocks can be defined as the constrained optimization problem.

In this problem, we can adjust only the amount of ballast water in each ballast tank. The design variable for this problem is the amount of water in 42 ballast water tanks, defined as Eq. 3.

$$\bar{\mathbf{B}} = (\bar{B}_1, \dots, \bar{B}_{42})^T \quad 0 \leq B_i \leq B_{\max,i} \quad (3)$$

where  $i = 1, 2, 3, \dots, 42$

The optimization problem using design variable  $\bar{\mathbf{B}}$  can be defined as below

$$\begin{aligned} \text{(p)} \quad & \min F(\bar{\mathbf{B}}) \\ \text{such that} \quad & g_j(\bar{\mathbf{B}}) \leq \varepsilon_j \\ \text{where} \quad & F(\bar{\mathbf{B}}), g_j(\bar{\mathbf{B}}): \mathfrak{R}^{42} \rightarrow \mathfrak{R} \end{aligned} \quad (4)$$

where  $F(\bar{\mathbf{B}})$  is an objective function,  $g_j$  are constraints, and  $j$  is the number of constraints.

### Constraints

There are several constraints on this problem to ensure the stability and safety of the OFD. The major constraints are trim, heel, and draft. According to problem definition:

$$\begin{aligned} g_1(\bar{\mathbf{B}}): & \text{Trim of OFD deck} \\ g_2(\bar{\mathbf{B}}): & \text{Heel of OFD deck} \\ g_3(\bar{\mathbf{B}}): & \text{Draft of OFD deck} \end{aligned}$$

The shape of the OFD is a curved surface in three dimensions. Location of the node in the FEM model is denoted by  $(x, y)$ . Moreover, value of the deformation at that location is denoted by  $z$ . We can configure deflection of OFD such as Fig. 5

The gradient along the  $x$ -direction is defined as the trim, in the  $y$ -direction as the heel. Because of difficulty of defining a gradient on a curved surface, we approximated a linear surface from the curved surface using linear regression (Jack, 2009). Thus, we can find trim and heel using Equations 5 and 6.

$$\bar{\mathbf{X}} = (1 \quad \bar{x} \quad \bar{y}), \quad \bar{\mathbf{Z}} = \text{FEM}(\bar{\mathbf{B}}) = (Z_1 \quad \dots \quad Z_{143})^T \quad (5)$$

$$\begin{bmatrix} 1 & g_1(\bar{\mathbf{B}}) & g_2(\bar{\mathbf{B}}) \end{bmatrix}^T = (\bar{\mathbf{X}}^T \times \bar{\mathbf{X}})^{-1} \times \bar{\mathbf{X}}^T \times \bar{\mathbf{Z}} \quad (6)$$

Another constraint is the draft. Draft refers to the average deformation of a whole node in the FEM model. Draft should maintain a certain value. Allowable values for constraints, which are expressed by  $\varepsilon_j$  in Eq.4, are presented in Table 1.

**Table 1: Allowable values for constraints of OFD**

Constraints	Symbol	Allowable error
Trim	$\varepsilon_1$	0.15
Heel	$\varepsilon_2$	0.15
Draft	$\varepsilon_3$	0.30 m

For solving the optimization problem, the values of constraints are noted in an objective function with the penalty method (Rao, 2009).

### Objective function

Depending on the type of erection, the objective function will change. Already mentioned in the structural model section, our research focused on step 8 in construction of the JSM. For this, the most important need for accuracy relates to the distance between columns. This distance influences the accuracy of the next erection step (raising the topside block on the columns).

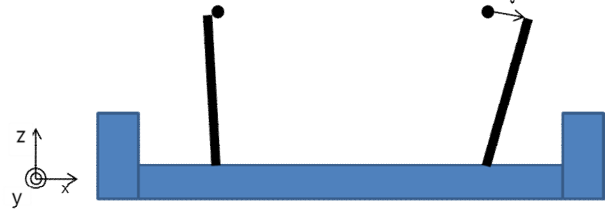


**Fig.6: Configuration of vector V**

As you see in Fig. 6, the thin lines are columns simulated by the FEM model, dots are right location of center of column's topside, and vector  $\vec{V}$  is defined by the angle and distance from the dot to the end of the thin line. The ideal objective function minimizes the vector  $\vec{V}$  of each column. Using the penalty method, a constraint function  $g_j$  is added to the objective function with a weight factor  $K_j$ . However, for the optimization problem we define the objective function as below:

$$F(\bar{\mathbf{B}}) = \sum_{i=1}^4 \vec{V} + K_1 \cdot g_1(\bar{\mathbf{B}}) + K_2 \cdot g_2(\bar{\mathbf{B}}) + K_3 \cdot g_3(\bar{\mathbf{B}}) \quad (7)$$

where

$K_i = 0$  (when  $g_i \leq \varepsilon_i$ ) or  $K_i = C$  (when  $g_i \geq \varepsilon_i$ ).  $C$  is a positive number greater than 1000.

### Steepest descent method

According to variations in the ballast water plan, the deformation of the OFD is continuous. The reason for this assumption is that actual operators of the OFD operate within linear elastic range for safety. The objective function can be differentiated due to the continuity of the OFD deformation. For this reason, we can use the steepest decent method to solve the optimization problem.

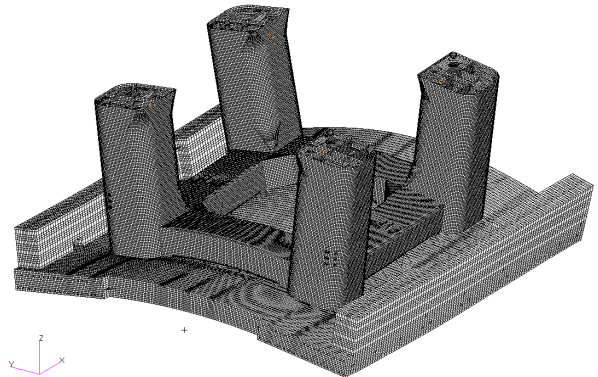


**Fig.7: Deflection of OFD by NASTRAN S/W**

A basic method for finding a local minimum is the steepest decent method. Cauchy (Rao, 2009) created this method in 1847, and it uses the negative gradient vector as a direction for minimization of the objective function. For this method, we start from an initial trial point (given by SHI) which is estimated using the NASTRAN FEM model (Fig. 7).

### Ending criteria

Since the time to solve the problem is limited, the number of iterations is also limited. The limited estimation time is limited to 5 min. When the estimation time exceeds 5 min, the proposed system stops the optimization procedure.

If  $F(\tilde{\mathbf{B}}_i) \leq \tau_1$  and  $\Delta = [F(\tilde{\mathbf{B}}_i) - F(\tilde{\mathbf{B}}_{i-1})]/F(\tilde{\mathbf{B}}_i) \leq \tau_2$ , the optimization procedure is ended, where  $\tau_1$  is tolerance for the objective function in Table 4, and  $\tau_2$  is the error value. Usually this error value is 0.1% and this value determines the speed of optimization.

### Metamodeling

There are differences between a simulation model, the FEM model in this research, and actual model. The usual way of compensating for these differences is by doing experiments with the actual model, and using the results to improve the simulation model. However, the OFD is a huge structure, so doing experiments costs a lot. Moreover, fixing the simulation model is not easy to do, and is also hard to implement.

Therefore, our research used metamodeling. Metamodeling is model approximation. Approximation of a global model, or some special part of a model, is used to reduce computation costs. In this way, engineers can easily understand the behavior or tendency of the model. Some known metamodel methods include Kriging,

response surfaces, surrogates, emulators, and auxiliary models. Our research team chose Ordinary Kriging (Olea, 1999) that is the simplest type of Kriging method. Ordinary Kriging assumes

$$\hat{y} = F(\mathbf{x}) + Z(\mathbf{x}) \quad (9)$$

where  $\hat{y}$  is the value of estimation by Kriging,  $\mathbf{x}$  is the vector of design variables,  $F(\mathbf{x})$  is the overall trend of the metamodel and  $Z(\mathbf{x})$  is deviation from a narrow area. The  $F(\mathbf{x})$  is expressed as a linear sum as in Eq. 10 with  $\beta_i$  as coefficient of  $f(\mathbf{x})$ .

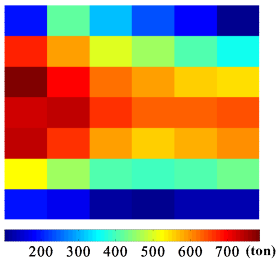
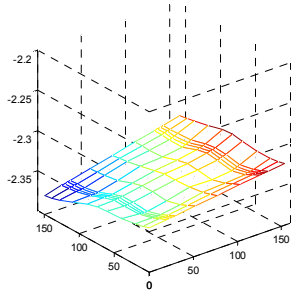
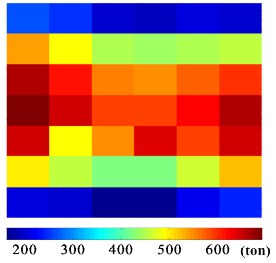
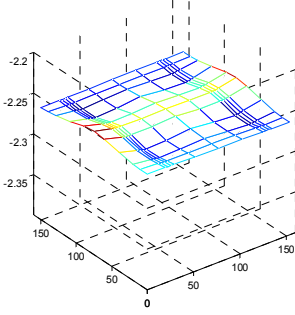
$$\begin{aligned} F(\mathbf{x}) &= \beta_1 f_1(\mathbf{x}) + \dots + \beta_p f_p(\mathbf{x}) \\ &= \begin{bmatrix} f_1(\mathbf{x}) & \dots & f_p(\mathbf{x}) \end{bmatrix} \begin{bmatrix} \beta_1 \\ \dots \\ \beta_p \end{bmatrix} \\ &= \tilde{f}(\mathbf{x})^T \tilde{\beta} \end{aligned} \quad (10)$$

where  $Z(\mathbf{x})$  is a Gaussian random process with zero mean and  $\sigma^2$  variance.

### Result and future work

As shown as Fig. 9, the proposed system found an optimal solution for the erection process during step 8 in construction of the JSM. The object value decreased with each iteration. After the ninth iteration, the object value did not decrease any more, meaning that the proposed system found a local minimum. Moreover, this value (13.56 mm) was located within the scope of acceptable range for erection. Tables 2 and 3 show comparisons of the initial and final states of the OFD.

**Table 2: comparison between initial and final state**

Condition	Ballast plan	Deformation of OFD	Object Value
Initial state			69.22 mm
Final state			13.56 mm

In metamodeling, we randomly chose several measurement data sets for making the metamodel. In addition, another several data sets, which did not include the data sets used for making the metamodel, were used for verification of the metamodel.

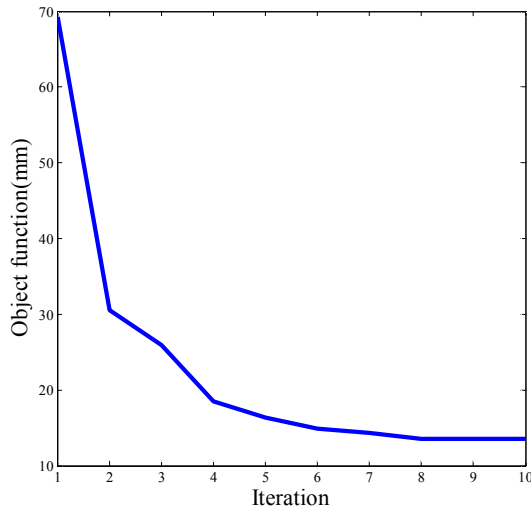


Fig. 9: Iteration vs. objective function

Table 3: Comparison accuracy of offshore blocks between initial state and final state

Condition	Initial state	Final state
Objective function	69.22 mm	13.56 mm
Trim	0.00015	0.000041
Heel	0.000012	0.000002

Fig.10 is the result of our metamodeling. In this figure, error means the difference in the object values provided by the metamodel and by the measurement data. The average error was 4.74%. The trend of the metamodel was similar to that of the measurement data. This meant that our metamodel had enough accuracy to apply to the optimization model.

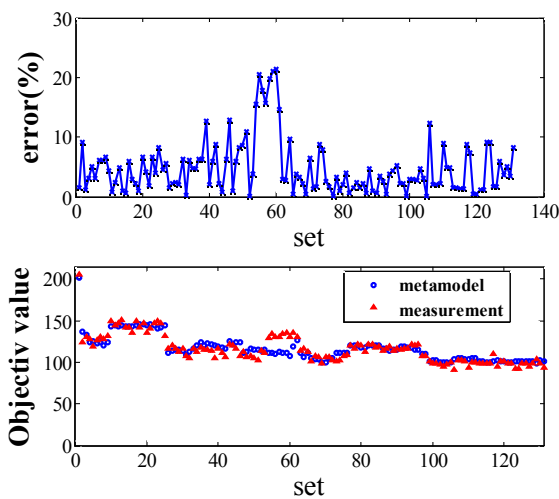


Fig. 10: result of metamodel

The proposed system was implemented on the OFD during erection of the JSM from February to June of 2012. The proposed system successfully controlled the

accuracy of matching blocks during construction of the JSM. In Step 8 of the JSM erection, the critical accuracy for the distance between columns, already mentioned in the section on the objective function, is shown in Table 4.

Table 4: result of measurement

Item	Measurement	Tolerance
Distance bet. Columns	-10 ~ -24 mm	±25.0 mm

## Conclusion

In this paper, a ballast water plan optimization system was proposed to control the accuracy of offshore blocks being erected and matched on the OFD, to within the tolerance limits. The proposed system consists of two parts, (a) a simplified FEM model with beam and plate elements, and (b) optimization module with Kriging.

The proposed system was used from February to June 2012, during erection of the JSM offshore platform on the OFD. The system successfully predicted the optimal ballast plans during the erection processes. Moreover, this system greatly helped SHI in erecting the JSM offshore structure, by improving control of the accuracy of the erection process.

## Reference

- Adi Kurniawan, and Guowei Ma (2009). "Optimization of ballast plan in launch jacket load-out", Struct Multidisc Optim, Vol 38, pp 267-288.
- Bathe K.J. (1996), "Finite element procedures", Prentice Hall.
- Lee P.S. and Bathe K.J. (2005), "Insight into finite element shell discretizations by use of the basic shell mathematical model", Comp Struct, Vol 83, pp 69-90.
- Yoon K, Lee Y.G. and Lee P.S. (2012), "A continuum mechanics based beam finite element with warping displacements and its modeling capabilities", Stuct Eng Mech Vol 43, pp 411-437
- Park KC, Felippa CA and Rebel G. (2002), "A simple algorithm for localized construction of nonmatching structural interfaces", Int.J. Numer. Methods Engng, Vol 53, pp 2117-2142
- Jack P.C. Kleijnen (2009), "Kriging metamodeling in simulation: A review", European Journal of Operational Research, Vol 192, pp 707-716
- Rao, S. S. (2009). "Engineering optimization: theory and practice.", Wiley.
- Olea, R. A. and Olea, R. A. (1999). "Geostatistics for engineers and earth scientists" Kluwer Academic Publishers.